THE JOURNAL OF BIOLOGICAL CHEMISTRY
Vol. 279, No. 2, Issue of January 9, pp. 1020–1029, 2004

Printed in U.S.A.

Protein Sorting in the Late Golgi of *Saccharomyces cerevisiae* Does Not Require Mannosylated Sphingolipids*

Received for publication, June 10, 2003, and in revised form, October 21, 2003
Published, JBC Papers in Press, October 28, 2003, DOI 10.1074/jbc.M306119200

Quirine Lisman‡§¶, Thomas Pomorski‖, Chantal Vogelzangs§, Dorothy Urli-Stam§, William de Cocq van Delwijnen‡, and Joost C. M. Holthuis‡**

From the ‡Department of Membrane Enzymology, Utrecht University Faculty of Chemistry, 3584 CH Utrecht, The Netherlands, the §Department of Cell Biology and Histology, Academic Medical Center, University of Amsterdam, 11085 AZ Amsterdam, The Netherlands, and the ‖Institut für Biologie, Humboldt-Universität zu Berlin, 10115 Berlin, Germany

Glycosphingolipids are widely viewed as integral components of the Golgi-based machinery by which membrane proteins are targeted to compartments of the endosomal/lysosomal system and to the surface domains of polarized cells. The yeast *Saccharomyces cerevisiae* creates glycosphingolipids by transferring mannose to the head group of inositol phosphorylceramide (IPC), yielding mannosyl-IPC (MIPC). Addition of an extra phosphoinositol group onto MIPC generates mannosyl-di-IPC ($M(IP)_2C$), the final and most abundant sphingolipid in yeast. Mannosylation of IPC is partially dependent on *CSG1*, a gene encoding a putative sphingolipid-mannosyltransferase. Here we show that open reading frame *YBR161w*, renamed *CSH1*, is functionally homologous to *CSG1* and that deletion of both genes abolishes MIPC and $M(IP)_2C$ synthesis without affecting protein mannosylation. Csg1p and Csh1p are closely related polytopic membrane proteins that co-localize with IPC synthase in the *medial*-Golgi. Loss of Csg1p and Csh1p has no effect on clathrin- or AP-3 adaptor-mediated protein transport from the Golgi to the vacuole. Moreover, segregation of the periplasmic enzyme invertase, the plasma membrane ATPase Pma1p and the glycosylphosphatidylinositol-anchored protein Gas1p into distinct classes of secretory vesicles occurs independently of Csg1p and Csh1p. Our results indicate that protein sorting in the late Golgi of yeast does not require production of mannosylated sphingolipids.

Correct sorting of membrane proteins and lipids is essential for establishing and maintaining the identity and function of the different cellular organelles. Although much progress has been made in uncovering the transport machinery for delivering endosomal/lysosomal proteins (1, 2), the mechanisms for cargo sorting to the cell surface are still poorly defined. Exocytic cargo can reach the cell surface by multiple pathways in most, if not all eukaryotic cells (3). For example, the polarized organization of epithelial cells relies on the sorting of both proteins and lipids into distinct classes of Golgi-derived vesicles that are targeted to the apical or basolateral surface (4). Apical and basolateral proteins expressed in fibroblasts are also sorted into different vesicles (5), and it appears that the Golgi-based sorting machinery for apical and basolateral cargo operates both in polarized and non-polarized cell types (6). Characterization of secretory vesicles that accumulate in late (post-Golgi-blocked) secretory yeast mutants has identified two vesicle populations with different densities and unique cargo proteins (7–9). Hence, transport of exocytic cargo by independent routes seems a conserved feature of eukaryotic cells.

There are numerous indications that lipid microheterogeneity plays a role in cargo sorting along the secretory pathway. Importantly, sphingolipids and in particular glycosphingolipids have the propensity to segregate from glycerolipids and to cluster with sterols into lateral microdomains with physicochemical properties distinct from those of the bulk membrane (10). Glycosphingolipid/sterol-rich microdomains were first conceived in polarized MDCK cells as Golgi-based sorting platforms for apically directed proteins and lipids (11, 12). In support of this model, inhibition of sphingolipid synthesis with fumonisin B randomizes the cell surface distribution of apical GPI[1]-anchored proteins in MDCK cells (13). A similar glycosphingolipid-based sorting mechanism is held responsible for axonal delivery of GPI-anchored proteins in neurons (14), regulated apical secretion of zymogens from pancreatic acinar cells (15), apical trafficking of thyroglobulin in thyrocytes (16), and cell surface delivery of plasma membrane ATPase, Pma1p, and diverse GPI-anchored proteins in yeast (17–19). Glycosphingolipids are also required for transport of melanosomal proteins from the Golgi to melanososomes in melanoma cells (20), but the underlying mechanism remains to be elucidated. The ubiquitous expression of glycosphingolipids suggests that they exert organizing functions in all eukaryotic cells.

Animals as well as some plants and fungi generate glycosphingolipids by transferring glucose or galactose to the C1 hydroxyl group of ceramide. These additions can be further decorated by additional sugars and sometimes sulfates to yield hundreds of different glycosphingolipid species (21). In the yeast *S. cerevisiae*, however, the direct precursor for glycosphingolipid synthesis is not ceramide but inositolphosphorylceramide (IPC, Ref. 22). IPC is formed by addition of phosphoinositol released from phosphatidylinositol to ceramide, a reaction catalyzed by IPC synthase in a *medial* compartment of

* The costs of publication of this article were defrayed in part by the payment of page charges. This article must therefore be hereby marked "*advertisement*" in accordance with 18 U.S.C. Section 1734 solely to indicate this fact.

This work is dedicated to Chantal Vogelzangs who set the basis of this study until her untimely death (June 24, 2000).

¶ Supported by a grant from the Meelmeijer foundation.

** Supported by a grant from the Royal Netherlands Academy of Arts and Sciences. To whom correspondence should be addressed: Dept. of Membrane Enzymology, Center for Biomembranes and Lipid Enzymology, H. R. Kruytgebouw N605, Padualaan 8, 3584 CH Utrecht, The Netherlands. Tel.: 31-30-253-6630; Fax: 31-30-252-2478; E-mail: j.c.holthuis@chem.uu.nl.

[1] The abbreviations used are: GPI, glycosylphosphatidylinositol; IPC, inositol phosphorylceramide; MIPC, mannosyl-IPC; HA, hemagglutinin; ORF, open reading frame; GFP, green fluorescent protein; ER, endoplasmic reticulum; CPY, carboxypeptidase Y; ALP, alkaline phosphatase.

the yeast Golgi (23). IPC is then mannosylated to yield mannosyl-IPC (MIPC), which in turn can receive a second phosphoinositol group from phosphatidylinositol to generate the final and by far most abundant sphingolipid, $M(IP)_2C$ (22). MIPC and $M(IP)_2C$ synthesis occurs in the lumen of the Golgi (22, 24). Whereas IPC is highly enriched in Golgi and vacuolar membranes, the largest amounts of MIPC and $M(IP)_2C$ are found in the plasma membrane (25). Hence, the yeast Golgi seems to be a branching point in sphingolipid trafficking from where mannosylated sphingolipids selectively migrate to the cell surface and sphingolipids without the sugar moiety reach the vacuole. However, direct evidence that mannosylated sphingolipids play a role in cargo sorting to the cell surface is lacking.

Addressing the biological function of mannosylated sphingolipids in yeast is hampered by the fact that little is known about the enzyme(s) responsible for their synthesis. Three structurally unrelated genes have been implicated in the mannosylation of IPC. The *VRG4* gene encodes a nucleotide sugar transporter that mediates GDP-mannose import into the Golgi lumen (24). Besides being essential for IPC mannosylation, *VRG4* also affects *N*-linked and *O*-linked glycoprotein modifications (24). Null mutations in either the *CSG1* or *CSG2* gene cause a reduction in, but do not completely eliminate MIPC synthesis (26, 27). Csg1p is predicted to have a catalytic function since it contains a region of 93 amino acids with homology to the yeast α-1,6-mannosyltransferase, Och1p (27). The function of Csg2p is less obvious. Csg2p contains an EF-Ca^{2+}-binding domain and has been localized to the ER where it may play a role in Ca^{2+} homeostasis (28). The recent finding that Csg2p forms a complex with Csg1p raises the possibility that IPC mannosyltransferase activity in yeast is regulated by Ca^{2+} through Csg2p (29).

Yeast open reading frame *YBR161w*, recently renamed *CSH1*, encodes a protein exhibiting strong similarity to the putative sphingolipid mannosyltransferase, Csg1p (27, 29). Here we report that Csh1p is functionally homologous to Csg1p and provide evidence that Csg1p and Csh1p function as two independent sphingolipid mannosyltransferases. Loss of Csg1p and Csh1p had no effect on the delivery of vacuolar proteins or on the packaging of cell surface components into distinct classes of secretory vesicles. From these results, we conclude that the organization of the various post-Golgi delivery pathways in yeast does not depend on production of mannosylated sphingolipids.

EXPERIMENTAL PROCEDURES

Strains and Plasmids—Unless indicated otherwise, yeast strains were grown at 28 °C to mid-logarithmic phase (0.5–1.0 OD_{600}) in synthetic dextrose (S.D.) medium or in yeast extract-peptone-dextrose (YEPD) medium. Yeast transformations were carried out as described (30). The yeast mutants Δ*pep12*Δ*vam3*, Δ*anp1*, Δ*mnn10* and Δ*van1* were all derived from the strain SEY6210 (*MATα ura3-52 his3* Δ200 *leu2-3-112 trpl-*Δ*901 suc2-*Δ*9 lys2-801*) and have been described elsewhere (31, 32). All other gene deletion phenotypes were characterized in the strain EHY227 (*MATα sec6-4 TPI1::SUC2::TRP1 ura3-52 his3* Δ*200 leu2-3-112 trp1-1*). For the deletion of *CSG1*, *CSH1*, and *IPT1* genes, 450–550 base pair fragments of the promoter and ORF 3′-end of each gene were amplified by PCR from yeast genomic DNA. The gene promoters and ORF ends were cloned into NotI/EcoRI and SpeI/MluI sites located on either site of a *loxP-HIS3-loxP* cassette that was ligated into the EcoRI/SpeI sites of a pBluescript KS^- vector (Stratagene, La Jolla, CA; the *loxP-HIS3-loxP* plasmid was a gift of T. Levine, University College London, UK). Gene deletion constructs were linearized with NotI and MluI and transformed into EHY227 to generate Δ*csg1* (JHY075), Δ*csh1* (JHY088), and Δ*ipt1* (JHY079) strains. Double deletions were performed sequentially in EHY227 by repeated use of the *loxP-HIS3-loxP* cassette and subsequent removal of the *HIS3* marker by excisive recombination using Cre recombinase (33), yielding the Δ*csg1*Δ*csh1* strain (JHY090). In each case, the correct integration or excision event was confirmed by PCR.

Aur1p was tagged at its C terminus with three copies of the hemagglutinin (HA) epitope using the PCR knock-in approach (34) and plasmid p3xHAt-HIS5 (S. Munro, MRC-LMB, Cambridge, UK). Pma1p was tagged at its N terminus with one copy of the HA epitope using integration plasmid pRS305Δ51 as described (35). Vam3p was tagged at its N terminus with three copies of the HA epitope using integration plasmid pRS405$(HA)_3$VAM3 (B. Nichols, MRC-LMB, Cambridge, UK). Expression plasmids encoding Myc-tagged invertase, Myc-tagged Mnt1p and GFP-tagged Sed5p have been described previously (23).

Promoter regions (650 bp) and open reading frames of *CSG1* and *CSH1* were PCR-amplified from yeast genomic DNA and subsequently ligated into single copy vector pRS413 (CEN, *HIS3*) or multicopy vector pRS425 (2μ, *LEU2*) (36). A second version of these constructs was prepared, but then with 3 copies of the HA epitope fused to the C termini of *CSG1* and *CSH1*, using PCR.

Lipid Analysis—Exponentially grown cells (0.5 OD_{600}) were inoculated in 5 ml of S.D. medium containing 10 μCi *myo*-[^{3}H]inositol (16 Ci/mmol; ICN Biomedicals, Eschwege) and grown for 16 h at 30 °C. Cells were harvested by centrifugation, washed twice with 10 mM NaN_3 and lipids extracted by bead bashing in H_2O/methanol/chloroform (5:16:16). The organic extracts were dried and subjected to butyl alcohol/water partitioning. Lipids recovered from the butyl alcohol phase were deacylated by mild base treatment using 0.2 N NaOH in methanol. After neutralizing with 1 M acetic acid, lipids were extracted with chloroform and separated by TLC using chloroform/methanol/4.2 M NH_3 (9:7:3). The TLC plate was dipped in 0.4% 2,5-diphenyloxazol dissolved in 2-methylnaphthalene supplemented with 10% xylene (37) and ^{3}H-labeled lipids detected by fluorography using Kodak X-Omat S films exposed at −80 °C. Alternatively, ^{3}H-labeled lipids were detected by exposure to BAS-TR2040 imaging screens (Fuji, Japan) and read out on a BIO-RAD Personal Molecular Imager (BioRad, Hercules, CA).

Analysis of IPC Mannosyltransferase Activity in Cell Extracts—Exponentially grown Δ*csg1*Δcsh1 cells (2.5 OD_{600}) were inoculated in 50 ml S.D. medium containing 100 μCi *myo*-[^{3}H]inositol and then grown for 16 h at 30 °C. Cells were harvested by centrifugation, washed twice with 10 mM NaN_3, and lysed by bead bashing in lysis buffer (50 mM Hepes, pH 7.2, 10 mM $MnCl_2$, 1 mM NEM) in the presence of fresh protease inhibitors. After removal of unbroken cells (500 × *g*, 10 min), membranes were collected (100,000 × *g*, 60 min) and solubilized in 1 ml of lysis buffer containing 1% and fresh protease inhibitors. After incubation for 60 min at room temperature, the extract was centrifuged (100,000 × *g*, 60 min), and 50-μl aliquots were stored at −80 °C. In addition, 400 OD_{600} of non-radiolabeled, exponentially-grown wild-type or Δ*csg1*Δcsh1 cells transformed with multicopy *CSG1*, *CSH1*, or control plasmids were lysed by bead bashing in 4 ml of ice-cold lysis buffer containing fresh protease inhibitors. Upon removal of unbroken cells, total membranes were collected, resuspended in 1 ml of ice-cold lysis buffer containing 1% Triton X-100, and rotated at 4 °C for 60 min.

For IPC mannosyltransferase assays, 50 μl of radiolabeled extract was mixed with 150 μl of unlabeled extract and then preincubated with 10 mM GDP-mannose (Sigma-Aldrich) for 10 min at 30 °C. Reactions were diluted 10-fold in lysis buffer and then incubated for 2 h at 30 °C. Reactions were stopped by adding 6.4 ml of chloroform:methanol (1:2.2). Lipids were extracted, deacylated, and separated by TLC as above.

Antibodies and Immunoblotting—Peptides corresponding to C-terminal regions of Csg1p and Csh1p (Fig. 1) were synthesized and then coupled to a carrier before immunization of rabbits. The resulting antisera were affinity-purified against peptides coupled to NHS-activated Sepharose 4 Fast Flow according to instructions of the manufacturer (Amersham Biosciences). Affinity-purified antibodies were used at a dilution of 1:1000 for immunoblot analysis and at 1:250 for immunofluorescence microscopy. Rabbit polyclonal antibodies to CPY, Gos1p, Pep12p, Tlg1p, and Tlg2p were described previously (38). Rabbit polyclonal antibodies to Sso2p were provided by S. Keränen, (Biotechnology and Food Research, Espoo, Finland) and to Gas1p by H. Riezman (Sciences II, Geneve, Switzerland). The Myc epitope was detected with mouse monoclonal antibody 9E10 or with rabbit polyclonal antibodies (Santa Cruz Biotechnology) and the HA epitope with rat monoclonal antibody 3F10, mouse monoclonal antibody 12CA5 (Roche Applied Science) or rabbit polyclonal antibodies (Santa Cruz Biotechnology). For immunoblotting, all antibody incubations were carried out in phosphate-buffered saline containing 5% dried milk and 0.5% Tween-20. After incubation with peroxidase-conjugated secondary antibodies (Bio-Rad), blots were developed using a chemiluminescent substrate kit (Pierce). Chemiluminescent bands were quantified using a GS-710 calibrating imaging densitometer (BioRad) with QuantityOne software.

Immunofluorescence Microscopy—Exponentially grown cells were

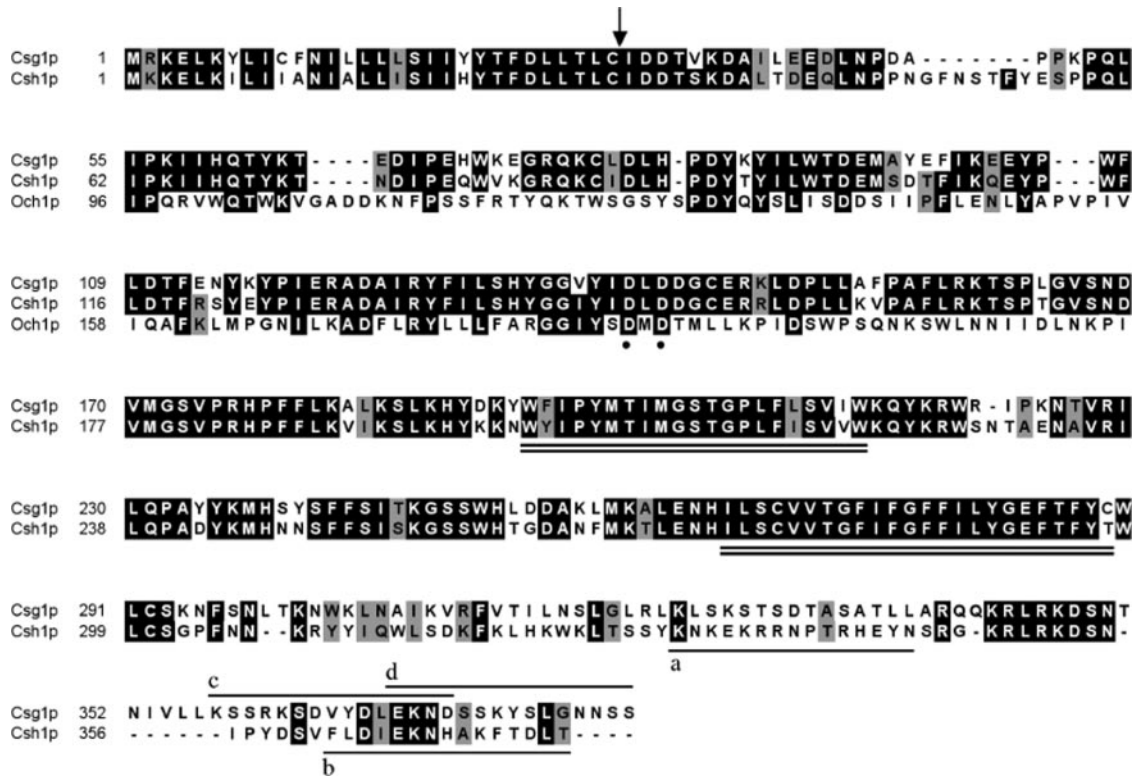

FIG. 1. **Alignment of the amino acid sequences of Csg1p, Csh1p, and Och1p.** Sequences were aligned with ClustalW. Conserved (*black*) or related residues (*gray*) are *boxed*. A putative signal peptide cleavage site is indicated by an *arrow*. Two potential transmembrane domains are doubly *underlined*. A conserved D*X*D motif found in many glycosyltransferases is marked by *dots*. *Single lines* (*a–d*) mark peptide sequences used to raise specific antibodies.

fixed and mounted on glass-slides as described previously (38). All antibody incubations were performed in phosphate-buffered saline supplemented with 2% dried milk and 0.1% saponin for 2 h at room temperature. Primary polyclonal antibodies to Csg1p, Csh1p, and the rat monoclonal 9F10 to HA were used at a dilution of 1:400, 1:150, and 1:250 respectively. Fluorescein- or Cy3-conjugated secondary antibodies (Amersham Biosciences) were used at a dilution of 1:100. Fluorescence microscopy and image acquisition were carried out using a Leica DMRA microscope (Leitz, Wetzlar, Germany) equipped with a cooled CCD camera (KX85, Apogee Instruments Inc., Tucson, AZ) driven by Image-Pro Plus software (Media Cybernetics, Silver Spring, MD).

Fractionation of Secretory Vesicles—Exponentially grown *sec6-4* cells expressing HA-tagged Pma1p (2.0 OD_{600}) were inoculated into YEPD medium (500-ml culture per gradient) and then grown for 14–16 h at 25 °C to 0.7 OD_{600}/ml. Next, cells were collected (500 × *g*, 5 min) resuspended in 250 ml of YEPD and then shifted to 38 °C for 60 min to induce the *sec6−4* secretory block. Spheroplasting, cell lysis, and collection of membrane pellet enriched in secretory vesicles (SVs) were performed essentially as described (7) except that SVs were collected on a 60% Nycodenz cushion in lysis buffer. SVs were resuspended in 1.5 ml of lysis buffer adjusted to 30% Nycodenz and then loaded at the bottom of a 11-ml linear 16–26% Nycodenz/0.8 M sorbitol gradient. Following centrifugation at 100,000 × g_{av} for 16 h min at 4 °C in a Beckman SW41Ti rotor, 0.6-ml fractions were collected from the top of the gradient. Fraction densities were determined by reading refractive indices on a Bausch and Lomb refractometer. Equal amounts per fraction were subjected to immunoblotting and analyzed for ATPase and invertase enzyme activity as described (7).

Immunoisolation of Secretory Vesicles—Immunoisolations of Pma1p-HA-containing SVs were performed using magnetic Dynabeads protein G (Dynal Biotech GmbH, Hamburg, Germany) loaded with mouse anti-HA (12CA5) or anti-Myc (9E10) monoclonal antibodies. Beads were incubated with antibodies for 40 min at room temperature and antibodies bound quantified by SDS-PAGE. Anti-HA beads contained 0.35 μg of 12CA5/μl of bead-slurry and control beads contained 0.1 μg of 9E10/μl bead-slurry. For immunoisolation of Pma1p-containing vesicles, a 300-μl reaction was prepared in lysis buffer containing 126 μl Dynabeads slurry, 5 mg/ml bovine serum albumin, and 15 μl membranes from Nycodenz gradient PM-ATPase peak fractions obtained by fractionating membranes derived from 1 g of cells. The reactions were rotated gently at 4 °C for 2 h. Supernatants were subjected to centrifugation (100,000 × *g*, 1 h, 4 °C), and membrane pellets were resuspended in 100 μl of SDS sample buffer. Beads were washed twice for 30 min in 1 ml of bovine serum albumin-containing lysis buffer, twice in lysis buffer, and resuspended in 75 μl of SDS sample buffer. Bound and unbound membranes were analyzed by immunoblotting.

RESULTS

CSH1 Encodes a Novel Putative IPC Mannosyltransferase—Comparative sequence analysis revealed that Csh1p is 67% identical to Csg1p and has the same predicted protein topology, namely a putative N-terminal signal sequence and two potential transmembrane segments localized to the C-terminal half of the protein (Fig. 1). Between the signal sequence and first transmembrane segment there is a region of 93 residues sharing 29% identity with the luminal portion (residues 96–197) of the yeast α-1,6-mannosyltransferase, Och1p (39). This region contains a conserved D*X*D motif that occurs in a wide range of glycosyltransferase families and likely forms part of a catalytic site (40).

Csg1p is required for accumulation of mannosylated sphingolipids in yeast and its similarity to Och1p suggests that the protein serves as an IPC mannosyltransferase (27). However, loss of Csg1p is not sufficient to abolish IPC mannosylation (see also below), raising the possibility that Csh1p represents an alternative IPC mannosyltransferase that functions independently of Csg1p. To investigate this possibility, we constructed yeast strains in which the ORFs of *CSG1*, *CSH1*, or both were removed. TLC analysis of alkaline-treated lipid extracts prepared from *myo*-[^{3}H]inositol-labeled cells showed that, compared with the wild-type strain, the Δ*csg1* mutant produced greatly reduced levels of the mannosylated sphingolipids MIPC and $M(IP)_2C$, and accumulated IPC-C and IPC-D (Fig. 2*A*, *lanes 1* and *2*; note that IPC-C contains a monohydroxylated C26 fatty acid whereas the C26 fatty acid in IPC-D is dihy-

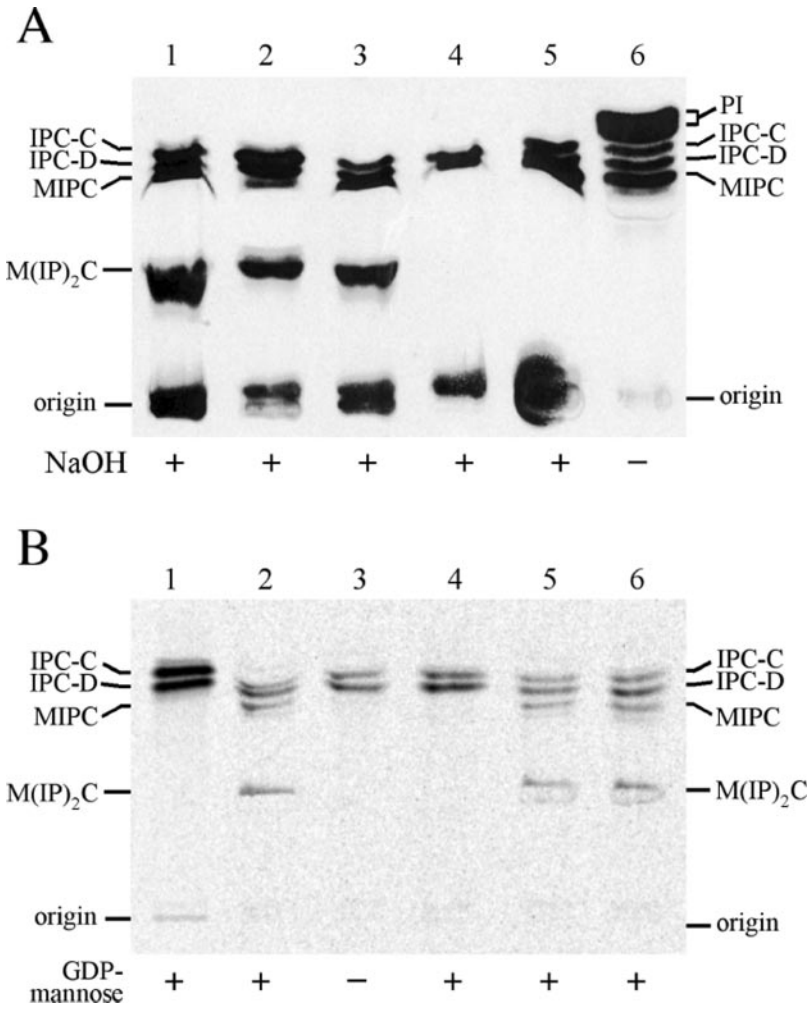

FIG. 2. **Csg1p and Csh1p have redundant functions in sphingolipid mannosylation.** *A*, deletion of *CSG1* and *CSH1* abolishes IPC mannosylation. Yeast cells were labeled overnight with *myo*-[^{3}H]inositol and the lipid extracts either deacylated by mild alkaline hydrolysis with NaOH (+) or control incubated (−). Lipids were extracted, separated by TLC, and then visualized by autoradiography as described under "Experimental Procedures." *Lane 1*, wild-type; *lane 2*, Δ*csg1*; *lane 3*, Δ*csh1*; *lane 4*, Δ*csg1*Δ*csh1*; *lanes 5* and *6*, Δ*ipt1*. Note that *IPT1* is known to have an essential function in $M(IP)_2C$ synthesis. *B*, analysis of IPC mannosyltransferase activity in Triton X-100 extracts derived from wild-type and Δ*csg1*Δcsh1 cells. Extracts prepared from *myo*-[^{3}H]inositol-labeled Δ*csg1*Δcsh1 cells were either control-incubated (*lane 1*) or mixed with extracts of unlabeled wild-type cells (*lanes 2* and *3*), Δ*csg1*Δcsh1 cells (*lane 4*), or Δ*csg1*Δcsh1 cells transformed with a multicopy vector containing *CSG1* (*lane 5*) or *CSH1* (*lane 6*). Incubations were performed in the presence (+) or absence (−) of 1 mM GDP-mannose as described under "Experimental Procedures." Lipids were extracted, deacylated, and then separated by TLC before autoradiography.

droxylated; (41). Unlike Δ*csg1* cells, the Δ*csh1* mutant produced IPC and mannosylated IPC species at ratios similar to those in wild-type cells (Fig. 2*A*, *lanes 1* and *3*). In the Δ*csg1*Δ*csh1* double mutant, however, production of MIPC and $M(IP)_2C$ was completely abolished (Fig. 2*A*, *lane 4*). These results are consistent with those reported in a recent study (29) and indicate that Csg1p and Csh1p have redundant functions in IPC mannosylation.

The block in MIPC and $M(IP)_2C$ synthesis observed in Δ*csg1*Δ*csh1* cells can be explained by a complete loss of IPC mannosyltransferase activity, but may also be due to a defective delivery of IPC or GDP-mannose to the transferase-containing compartment. To explore these possibilities, we analyzed the IPC mannosyltransferase activity in detergent extracts derived from wild-type and Δ*csg1*Δ*csh1* cells. To this end, Triton X-100 extracts prepared from *myo*-[^{3}H]inositol-labeled Δ*csg1*Δ*csh1* cells were mixed with extracts from unlabeled wild-type or mutant cells, and then incubated in the presence or absence of externally added GDP-mannose. When extracts from inositol-labeled Δ*csg1*Δ*csh1* cells were incubated with unlabeled wild-type cell extracts, radioactive IPC was converted to MIPC and $M(IP)_2C$ in a GDP-mannose-dependent manner (Fig. 2*B*, *lanes 2* and *3*). In contrast, addition of GDP-mannose to Δ*csg1*Δ*csh1* cell extracts was not sufficient to support MIPC and $M(IP)_2C$ synthesis (Fig. 2*B*, *lanes 1* and *4*). However, when inositol-labeled Δ*csg1*Δ*csh1* extracts were incubated with extracts from unlabeled Δ*csg1*Δ*csh1* cells transformed with the *CSG1* or *CSH1* gene on a multicopy plasmid, the GDP-mannose-dependent mannosylation of IPC was restored (Fig. 2*B*, *lanes 5* and *6*).[2] These results indicate that Δ*csg1*Δ*csh1* cells are defective in IPC mannosyltransferase activity rather than in IPC or GDP-mannose transport.

To investigate whether loss of Csg1p and Csh1p also affects protein mannosylation, we next examined the glycosylation state of invertase produced in wild-type and mutant strains. This periplasmic enzyme undergoes extensive outer chain mannan addition on 8–10 of its *N*-linked glycans while passing through the Golgi (42). Consequently, its electrophoretic mobility is increased when enzymes responsible for mannan synthesis are removed (32, 43). Immunoblot analysis of cells expressing Myc-tagged invertase showed that the gel mobility of the protein produced in the Δ*csg1*Δ*csh1* mutant was indistinguishable from that in wild-type cells (Fig. 3, *lanes 1* and *3*). In contrast, loss of mannosyltransferases involved in the initiation (Van1p) or elongation (Anp1p, Mnn10p) of the mannan backbone caused a substantial increase in the gel mobility of invertase (Fig. 3, *lanes 4–6*). These results demonstrate that protein mannosylation occurs independently of Csg1p and Csh1p, and that the defect in sphingolipid mannosylation in Δ*csg1*Δ*csh1* cells is specific.

Collectively, our results suggest that yeast contains two independent IPC mannosyltransferases: one encoded by *CSG1* and likely responsible for producing the bulk of mannosylated IPC, and the second one encoded by *CSH1* and corresponding to a minor IPC mannosyltransferase activity.

[2] Q. Lisman and J. C. M. Holthuis, unpublished data.

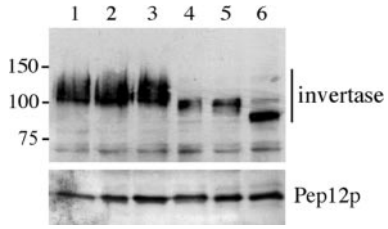

FIG. 3. **Loss of Csg1p and Csh1p does not affect protein mannosylation.** An immunoblot of total protein extracts prepared from wild-type and various mannosyltransferase mutant cells expressing Myc-tagged invertase was stained with a monoclonal antibody to the Myc epitope. The blot was reprobed with polyclonal antibodies to the endosomal t-SNARE, Pep12p, to control for equal loading. The positions of size markers (kDa) are indicated. *Lane 1*, wild-type; *lane 2*, Δ*csg1*; *lane 3*, Δ*csg1*Δcsh1; *lane 4*, Δanp1; *lane 5*, Δ*mnn10*; *lane 6*, Δ*van1*.

Membrane Topology of Csg1p and Csh1p—Golgi-associated glycosyltransferases generally have a type II topology with a short cytoplasmic tail and a large catalytic domain in the lumen (*e.g.* Mnt1p). Csg1p and Csh1p, on the other hand, contain a putative N-terminal signal sequence and two potential membrane spans that predict a different membrane topology where both termini of the protein are situated in the lumen (Fig. 4*A*). To test this prediction, we introduced three copies of the HA epitope at the C terminus of Csg1p. Attachment of the epitope did not inactivate the enzyme since expression of Csg1p-HA restored production of mannosylated sphingolipids in Δ*csg1*Δ*csh1* cells (data not shown). Expression of Csg1p-HA resulted in the appearance of two major protein bands of ~48 and 54 kDa on blots of total yeast extracts probed with anti-HA antibody (Fig. 4*B*, *lane 2*). Pretreatment of extracts with endoglycosidase F (Endo F) abolished the 54-kDa band and increased the intensity of the 48-kDa band (Fig. 4*B*, *lane 3*), indicating that a portion of Csg1p is glycosylated on one or more asparagine residues. Since all 5 potential *N*-linked glycosylation sites of Csg1p occur within its hydrophilic C terminus (see Fig. 1), this region would be luminal. Indeed, when membranes from cells expressing Csg1p-HA were treated with trypsin, the 48 and 54-kDa protein bands were degraded and a major HA-tagged product of 24 kDa appeared in the absence of detergent (Fig. 4*C*). Under these conditions, the *medial*-Golgi v-SNARE Gos1p was degraded whereas removal of a luminal, C-terminal Myc tag fusion to the type II Golgi enzyme Mnt1p was observed only after detergent treatment. Together, these findings demonstrate that the C terminus of Csg1p is luminal, hence consistent with the topology depicted in Fig. 4*A*.

Csg1p and Csh1p Co-localize with IPC Synthase to the medial-Golgi—To investigate the subcellular distribution of Csg1p and Csh1p, we raised polyclonal antibodies against synthetic peptides corresponding to areas with the least sequence homology (see Fig. 1). Antibodies against Csg1p-derived peptides detected 45- and 52-kDa protein bands on immunoblots of wild-type yeast extracts. These bands were absent in extracts from Δ*csg1* mutant strains while their levels increased 10-fold in cells expressing Csg1p from a multicopy vector (Fig. 5*A*). Antibodies against Csh1p-derived peptides detected a 48-kDa band, but only in extracts of cells over-expressing Csh1p from a multicopy vector (Fig. 5*A*). We initially investigated the subcellular distribution of Csg1p and Csh1p by fractionating organelles from wild-type yeast on equilibrium sucrose density gradients and blotting the gradient fractions with the specific antibodies. Csg1p and Csh1p clearly separated from markers for late Golgi/early endosomes (Kex2p, Tlg1p, Tlg2p), vacuoles (Vam3p) and plasma membrane (Sso2p; Fig. 5*B* and data not shown). In contrast, Csg1p and Csh1p co-fractionated with the *medial*-Golgi v-SNARE Gos1p, with IPC synthase activity and with HA-tagged Aur1p, a protein required for IPC synthesis and localized to the *medial*-Golgi (23, 44).

Since the different compartments of the yeast Golgi are not well resolved on sucrose gradients, the localization of Csg1p and Csh1p was further investigated by immunofluorescence microscopy. Staining of wild-type cells with anti-Csg1p antibodies produced a punctate pattern characteristic of the yeast Golgi apparatus that was absent in Δ*csg1* cells (Fig. 6*A*). A similar pattern was observed when cells were stained with anti-Csh1p antibodies, but only when Csh1p was overexpressed from a multicopy vector. These Csh1p-positive structures showed extensive co-localization with HA-tagged Csg1p, indicating that the two proteins occupy the same subcompartment of the Golgi (Fig. 6*B*). There was no significant co-localization of Csg1p/Csh1p-labeled spots with GFP-tagged Sed5p, a marker of the *cis* Golgi (Fig. 7). However, Csg1p/Csh1p-positive structures showed substantial co-localization with HA-tagged Aur1p (Fig. 7) and with the *medial*-Golgi marker Mnt1p (data not shown).

To verify co-localization of Csg1p/Csh1p and Aur1p by a complementary method, cells expressing Aur1p with three copies of the HA epitope inserted at its cytosolic C terminus were lysed and Aur1p-containing membranes immunoisolated using anti-HA antibodies bound to magnetic beads. This method allowed the isolation of nearly 20% of the Aur1p-HA containing membranes from a cell lysate (Fig. 8*A*). Strikingly, a similar fraction of Csg1p-containing membranes was bound to the beads. Binding of Aur1p-HA- and Csg1p-containing membranes was strictly dependent on the presence of anti-HA antibodies on beads. Membranes containing the ER marker Dpm1p did not bind. As additional control, the immunoisolation procedure was repeated on lysates of cells expressing the HA-tag on the cytosolic N terminus of the vacuolar *t*-SNARE, Vam3p. As shown in Fig. 8*B*, anti-HA beads brought down nearly half of the Vam3p-containing membranes. Under these conditions, neither Csg1p- nor Dpm1p-containing membranes did bind. Collectively, our results indicate that Csg1p and Csh1p primarily reside with the IPC synthase in a *medial* compartment of the yeast Golgi.

Golgi-to-Vacuole Transport Pathways Are Unaffected in Mutants Deficient in Mannosylated Sphingolipids—In mammals, glycosphingolipids have been implicated in targeting membrane proteins from the Golgi to compartments of the endosomal/lysosomal system (20) and to the surface domains of polarized cells (12–15). To investigate whether mannosylated sphingolipids in yeast serve a similar role, the Δ*csg1*Δ*csh1* mutant was analyzed for possible defects in post-Golgi delivery pathways.

In yeast, biosynthetic transport of proteins from the Golgi to the vacuole proceeds through two separate pathways, the carboxypeptidase Y (CPY) pathway and the alkaline phosphatase (ALP) pathway. Whereas the CPY pathway mediates a clathrin-dependent delivery of vacuolar proteins via late (prevacuolar) endosomes, the ALP pathway provides an alternative, clathrin-independent route that bypasses late endosomes and requires the AP-3 adaptor protein complex (2). The vacuolar protease CPY is synthesized as a p1 precursor in the ER, modified to a slightly larger p2 form in the Golgi, and then passes through late endosomes to reach the vacuole where it is proteolytically processed to its mature form (45). Pulse-chase immunoprecipitation analysis revealed that CPY maturation in the Δ*csg1*Δ*csh1* mutant is unaffected (Fig. 9). The efficient processing of CPY indicated that there was little mis-sorting to the cell surface, and indeed we failed to detect any radiolabeled CPY released from Δ*csg1*Δ*csh1* cells. This is in contrast to cells lacking the endosomal/vacuolar syntaxins Pep12p and Vamp3p where CPY is diverted to the cell surface in the p2 form (Fig. 9).

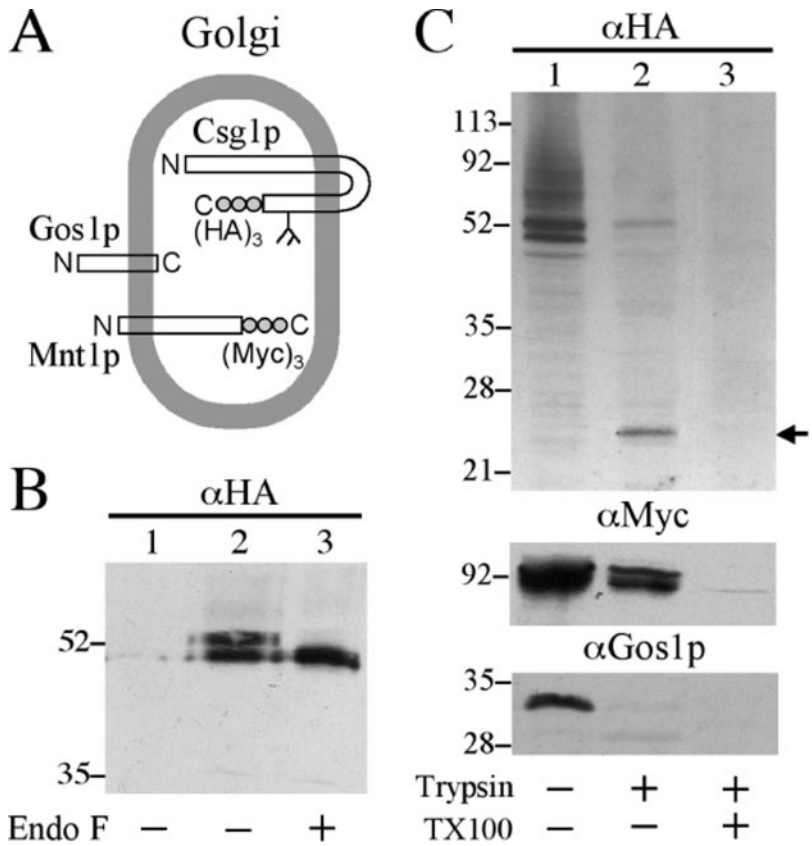

FIG. 4. **Membrane topology of Csg1p.** *A*, schematic view of the (predicted) membrane topologies of Golgi v-SNARE, Gos1p, glycosyltransferase, Mnt1p, and putative sphingolipid mannosyltransferase, Csg1p. *B*, total protein extracts from cells in which Csg1p was either tagged with three copies of the HA epitope (*lanes 2* and *3*) or not (*lane 1*) were treated for 24 h at 37 °C with 80 mU EndoF (Roche Applied Science) per 60 μg of protein, as indicated. Proteins were resolved by SDS-PAGE and subjected to Western blot analysis using anti-HA antibodies. *C*, immunoblot of membranes from yeast cells expressing Csg1p and Mnt1p tagged with three copies of the HA (Csg1p) or Myc epitope (Mnt1p) at the C terminus. Membranes were pretreated for 30 min at 30 °C with 8 mM trypsin and 0.4% Triton X-100 (*TX100*), as indicated. Each lane contains membranes prepared from 33 OD (600 nm) units of log-phase grown cells, as described previously (38). The immunoblot was stained with polyclonal antibodies against the HA epitope, the Myc epitope, or the Golgi v-SNARE, Gos1p.

The vacuolar membrane protein ALP is synthesized as a precursor that undergoes proteolytic processing in the vacuole yielding a smaller mature form (46). As shown in Fig. 9, Δ*csg1*Δ*csh1* cells displayed no significant delay in ALP maturation. In the Δ*pep12*Δ*vam3* mutant, on the other hand, ALP maturation was abolished. These results show that mannosylated sphingolipids in yeast do not serve a critical function in clathrin- or AP-3-mediated protein transport from the Golgi to the vacuole. Moreover, the efficient processing of newly synthesized CPY and ALP in Δ*csg1*Δ*csh1* cells indicates that blocking sphingolipid mannosylation has no general effect on forward transport through the Golgi apparatus. Consistent with this notion, Δ*csg1*Δ*csh1* and wild-type cells contain similar amounts of Golgi-modified invertase (Fig. 3).

Mannosylated Spingolipids Are Not Required for Sorting Cell Surface Proteins into Distinct Classes of Secretory Vesicles—The characterization of secretory vesicles that accumulate in late exocytic yeast mutants (*e.g. sec1*, *sec6*) has identified two vesicle populations with different densities and distinct cargo proteins, indicating the existence of two parallel routes from the Golgi to the plasma membrane (7–9). The more abundant, lighter density vesicles contain the major plasma membrane ATPase Pma1p whereas the denser vesicles contain the periplasmic enzymes invertase and acidic phosphatase. Sorting invertase into the dense class of vesicles requires clathrin and an intact Golgi-to-late endosome transport pathway (9, 47). From these observations, it has been suggested that invertase is sorted from Pma1p at the late Golgi for delivery to late endosomes, from where high-density vesicles bud that carry invertase to the cell surface.

To investigate whether mannosylated sphingolipids play a role in the organization of membrane trafficking to the cell surface, we disrupted the *CSG1* and *CSH1* genes in the late secretory mutant *sec6-4* and analyzed the strain for defects in secretory cargo sorting. The *sec6-4* strain harbors a temperature-sensitive mutation in a component of the exocyst protein complex that is required for polarized fusion of exocytic vesicles with the plasma membrane (48). The *sec6-4* mutant grows like wild-type cells at 25 °C, but growth ceases at 38 °C, and cells accumulate plasma membrane ATPase- and invertase-containing vesicles that can be separated by equilibrium isodensity centrifugation on Nycodenz gradients (7). To this end, *sec6-4* cells were grown at 25 °C, shifted to 38 °C for 90 min, lysed and then subjected to a 13,000 × *g* spin to remove most of the ER, nuclei, vacuoles, mitochondria, and plasma membrane. Next, a high-speed (100,000 × *g*) membrane pellet enriched in secretory vesicles was collected and loaded at the bottom of a linear 16–26% Nycodenz gradient in 0.8 M sorbitol. As shown in Fig. 10, gradient fractionation of membranes from 38 °C-shifted cells resulted in two peaks of enzyme activities that were absent when fractionation was performed on 25 °C-grown cells: a low density peak (fractions 4–9) containing ATPase activity and a higher density peak (fractions 10–15) containing invertase activity (note that the invertase peak found near the bottom of the gradient (fractions 17–20) likely corresponds to the cytoplasmic, non-glycosylated form of the enzyme). Western blot analysis revealed that Pma1p co-fractionates with the lower density membranes, confirming that the detected ATPase activity is due to this protein. In contrast, markers for the ER (Dpm1p) and Golgi (Gos1p) did not peak with either vesicle population, and their levels in gradients of 25 °C grown and 38 °C shifted cells were very similar (Fig. 10 and data not shown). This indicates that the detected ATPase and invertase peaks are not due to the accumulation or fragmentation of the ER or Golgi apparatus.

The fractionation profiles of ATPase activity, Pma1p and invertase in gradients of 38 °C-shifted *sec6-4*Δ*csg1*Δ*csh1* cells closely resembled those found for *sec6-4* cells (Fig. 10). This shows that mannosylated sphingolipids are required neither for the biogenesis of the light or the dense class of secretory

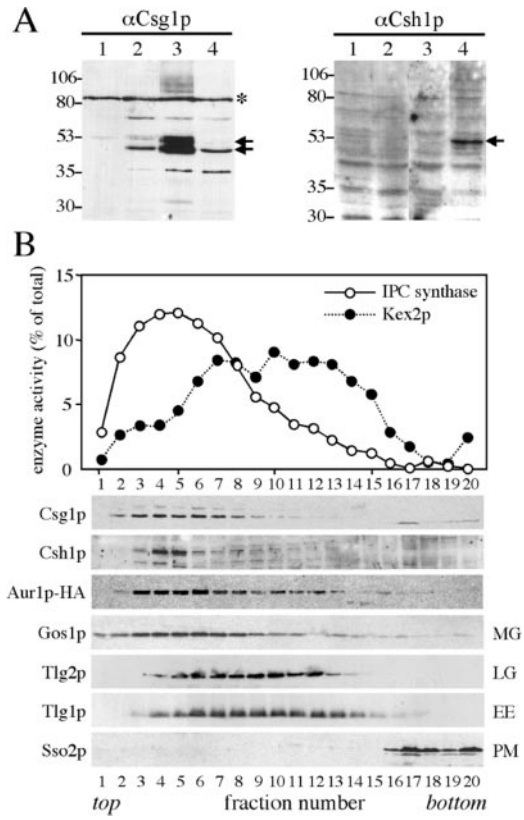

FIG. 5. **Subcellular fractionation of Csg1p and Csh1p.** *A*, immunoblots containing equal amounts of total protein extracts prepared from Δ*csg1* cells (*lane 1*), Δ*csh1* cells (*lane 2*), or wild-type cells transformed with a multicopy vector containing *CSG1* (*lane 3*) or *CSH1* (*lane 4*). Blots were stained with polyclonal anti-Csg1p or anti-Csh1p antibodies that were raised against synthetic peptides corresponding to areas with the least sequence homology (see Fig. 1). *B*, sucrose gradient fractionation of membranes. A high-speed membrane pellet (100,000 × *g*) prepared from yeast cells expressing HA-tagged Aur1p was fractionated on a sucrose density gradient. Fractions were assayed for IPC synthase and Kex2p enzyme activities as described under "Experimental Procedures." Fractions were also analyzed by immunoblotting using polyclonal antibodies against Csg1p, Csh1p and several organellar markers. A mouse monoclonal anti-HA antibody was used to detect HA-tagged Aur1p. *MG*, *medial*-Golgi; *LG*, late Golgi; *EE*, early endosomes; *PM*, plasma membrane.

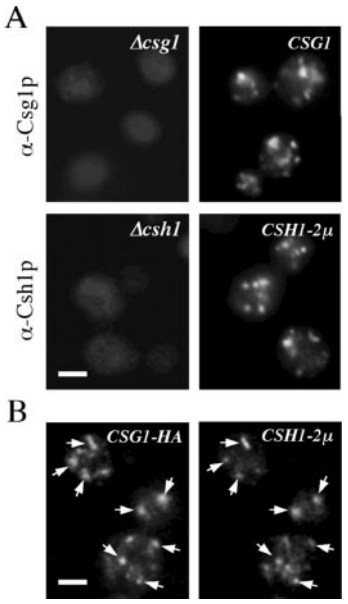

FIG. 6. **Colocalization of Csg1p and Csh1p by immunofluorescence.** *A*, immunofluorescence confocal micrographs of yeast cells stained with affinity-purified rabbit polyclonal antibodies directed against Csg1p (α-Csg1p) or Csh1p (α-Csh1p). Note that anti-Csg1p fluorescence is observed in wild-type (*CSH1*), but not in Δ*csg1* cells, whereas anti-Csh1p fluorescence occurs only in cells overexpressing Csh1p from a multicopy plasmid (*CSH1-2μ*). *B*, double-label immunofluorescence confocal micrographs comparing the localization of HA-tagged Csg1p (*CSH1-HA*) with Csh1p expressed from a multicopy plasmid (*CSH1–2μ*). Anti-HA staining was with rat monoclonal antibody 3F10. Most of the Csg1p-positive structures were also positive for Csh1p (*arrows*). *Bars*, 3 μm.

vesicles, nor for segregating Pma1p and invertase into these different vesicle populations. Since glycosphingolipids have previously been implicated in the sorting of GPI-linked proteins (13–15), we wished to determine which of the two secretory vesicle classes in yeast mediates transport of the GPI-anchored cell surface protein Gas1p. Western blot analysis revealed that Gas1p co-fractionates with Pma1p and ATPase activity in gradients of 38 °C-shifted *sec6-4* cells, regardless of whether Csg1p and Csh1p were present (Fig. 10). A similar fractionation profile was observed for the GPI-linked protein Ysp1p (data not shown). The co-fractionation of GPI-linked proteins and Pma1p suggests that these proteins are packaged into a common carrier. However, it is also possible that GPI-linked proteins are sorted into a different class of vesicles with fractionation properties similar to that of Pma1p-transporting vesicles. To distinguish between these possibilities, we immunoisolated Pma1p-containing vesicles from 38 °C-shifted *sec6-4* and *sec6-4*Δ*csg1*Δ*csh1* cells, and assessed whether these vesicles contained Gas1p. Immunoisolations were performed with membranes derived from 38 °C-shifted cells expressing Pma1p with three copies of the HA epitope inserted at its cytosolic N terminus. Membranes were fractionated on a Nycodenz gradient as above and Pma1p-HA containing vesicles isolated from the ATPase peak fraction (fraction 7) using anti-HA monoclonal antibodies bound to magnetic beads. This allowed the isolation of about 70% of Pma1p-HA and 50% of Gas1p present in the *sec6–4* ATPase peak fraction (Fig. 11). Immunoisolation of Pma1p-HA from the *sec6-4*Δ*csg1*Δ*csh1*-derived ATPase peak was less efficient (24% total), but brought down a similar portion of Gas1p (16%). In both cases, binding of Pma1p-HA and Gas1p containing membranes was strictly dependent on the presence of anti-HA antibodies on the beads. It therefore appears that Pma1p and Gas1p are packaged into a common transport carrier for delivery to the cell surface. Moreover, our findings demonstrate that sorting of GPI-linked proteins in the late secretory pathway of yeast essentially occurs independently of mannosylated sphingolipids.

DISCUSSION

The results presented in this study indicate that the yeast genes *CSG1* and *CSH1* encode proteins with a primary and redundant function in the mannosylation of phosphoinositol-containing sphingolipids. Our finding that Δ*csg1*Δ*csh1* cells exhibit a specific and complete block in sphingolipid mannosylation offered an opportunity to explore the potential role of mannosylated sphingolipids in secretory cargo sorting in yeast.

A primary function of Csg1p and Csh1p as sphingolipid mannosyltransferases is supported by the following observations. First, removal of Csg1p and Csh1p suffices to abolish MIPC and $M(IP)_2C$ synthesis, resulting in accumulation of MIPC precursor, IPC. Second, biochemical characterization of the IPC mannosyltransferase activity in cell extracts revealed that the inability of Δ*csg1*Δ*csh1* cells to generate MIPC and $M(IP)_2C$ can not be attributed to a defective delivery of GDP-mannose or IPC to the transferase-containing compartment. Third, Csg1p and Csh1p share a region of homology with the yeast α-1,6-mannosyltransferase Och1p and contain a con-

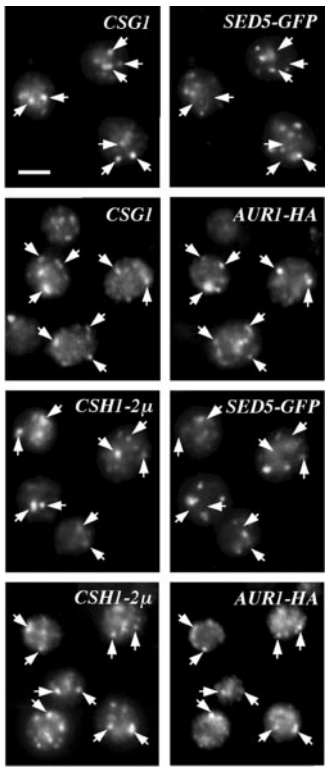

FIG. 7. **Csg1p and Csh1p colocalize with Aur1p by immunofluorescence.** Double-label immunofluorescence confocal micrographs comparing the localization of Csg1p and Csh1p with that of GFP-tagged Sed5p (*cis* Golgi) or HA-tagged Aur1p (*medial*-Golgi). Staining of Csg1p and Csh1p was performed as in Fig. 6 with Csh1p expressed from a multicopy plasmid (*CSH1-2μ*). Staining of HA-tagged Aur1p was with the rat mAb, 3F10. Csg1p and Csh1p positive structures were often positive for Aur1p, but not for Sed5p. *Bar*, 5 μm.

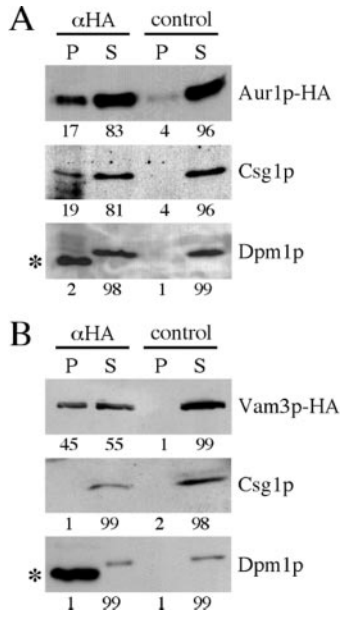

FIG. 8. **Membranes immunoisolated by Aur1p contain Csg1p.** High speed membrane pellets (100,000 × *g*) prepared from cells expressing 3 copies of the HA epitope on the cytosolic C terminus of Aur1p (*A*) or N terminus of vacuolar t-SNARE Vam3p (*B*) were subjected to immunoprecipitation using Dynabeads protein G preincubated with (αHA) or without (control) mouse anti-HA monoclonal antibody, 12CA5. Percentages of immunoprecipitated Aur1p, Vam3p, Csg1p, and the ER marker, Dpm1p, were determined by Western blot analysis using rabbit polyclonal antibodies against the HA-epitope or Smt1p, and a mouse monoclonal antibody against Dpm1p. Note that immunostaining against Dpm1p led to cross-reactivity with the 12CA5-derived IgG light chain (*asterisk*). *P*, beads; *S*, supernatant.

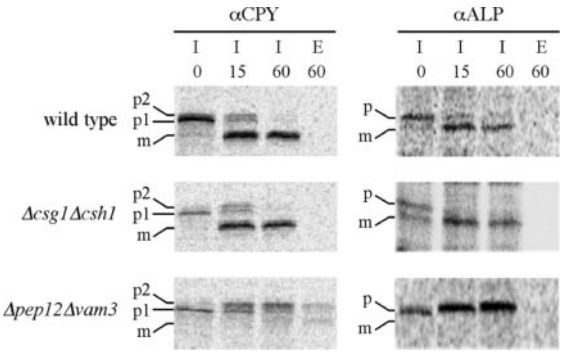

FIG. 9. **Vacuolar protein sorting and processing in the Δ*csg1*Δ*csh1* mutant.** Wild-type, Δ*csh1*Δcsg1, and Δ*pep12*Δvam3 cells were pulse-labeled with ^{35}S-labeled amino acids for 10 min, and then chased with nonradioactive methionine and cysteine for the indicated time points (min) at 26 °C as described previously (54). Carboxypeptidase Y (*CPY*) and alkaline phosphatase (*ALP*) were immunoprecipitated from lysed cells (*I*) and the medium (*E*), resolved by SDS-PAGE and visualized on a PhosphorImager. Precursor (*p*) and mature forms (*m*) of CPY and ALP are indicated.

served D*X*D motif, which is part of a catalytic site found in many known glycosyltransferases (40). Fourth, Csg1p and Csh1p are localized to the yeast Golgi where sphingolipid mannosylation is known to occur (49). Fifth, protease protection analysis and the utilization of *N*-linked glycosylation sites in Csg1p predict a membrane topology with the Och1p-homology domain and D*X*D motif positioned in the Golgi lumen, hence in keeping with the fact that sphingolipid mannosylation takes place on the luminal aspect of the Golgi (24).

Whether Csg1p and Csh1p are IPC mannosyltransferases or represent catalytic subunits of two distinct IPC mannosyltransferase complexes remains to be established. Recent work revealed that Csg1p and Csh1p occur in a complex with Csg2p, a putative Ca^{2+}-binding membrane protein lacking homology to glycosyltransferases. Several lines of evidence suggest that the role of Csg2p in these complexes is regulatory rather than enzymatic (29). In any case, the latter study and our present findings point to the existence of two independent IPC mannosyltransferases in yeast. So why would yeast need two distinct sphingolipid mannosyltransferases? We found that Csg1p and Csh1p are co-localized with IPC synthase to a *medial* compartment of the Golgi. Hence, the expression of two sphingolipid mannosyltransferases unlikely serves to accommodate a need for synthesizing mannosylated sphingolipids at different cellular locations. It should be noted that yeast IPC is not a monomolecular lipid species, but represents a mixture of molecules that differ in the chain length and the extent of hydroxylation of both the sphingoid base and fatty acid (22). This raises the possibility that the two IPC mannosyltransferases differ in substrate specificity. Indeed, metabolic labeling of Δ*csg1* and Δ*csh1* cells with [^{3}H]dihydrosphingosine revealed some differences in activity between Csg1p and Csh1p toward particular molecular species of IPC (29). The biological implications of this finding remain to be established.

A key function attributed to sphingolipids is their ability to self-associate into membrane microdomains/rafts, especially when sterols are present. Formation of sphingolipid/sterol-rich microdomains is important for lateral sorting of membrane proteins, in particular those containing a GPI anchor (50, 51). Previous work in yeast has shown that sphingolipid depletion affects both raft association and cell surface delivery of Pma1p and GPI-anchored proteins, *i.e.* Gas1p (17–19). In these studies, sphingolipid synthesis was blocked using a conditional allele of serine palmitoyltransferase activity, which catalyzes

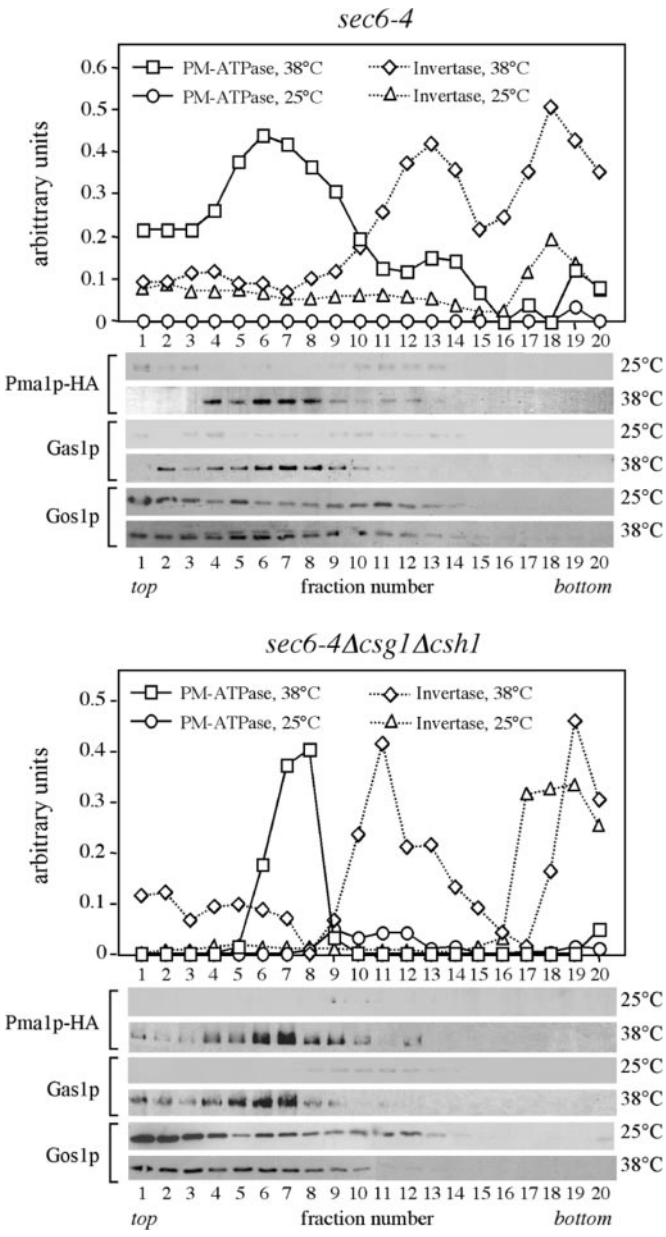

FIG. 10. **Gradient fractionation of secretory vesicles accumulated in *sec6-4* and *sec6-4Δcsg1Δcsh1* cells.** Membrane pellets (100,000 × *g*) enriched in secretory vesicles were prepared from temperature-shifted (38 °C) and non-shifted (25 °C) cells, loaded on the bottoms of linear 16–26% Nycodenz/0.8 M sorbitol gradients and then floated to equilibrium by centrifugation. Fractions were collected from the top and analyzed for enzyme activities and by immunoblotting. Enzyme activities are expressed in arbitrary units based upon the absorbance measured at 820 nm (*PM-ATPase*) or 540 nm (*invertase*) as described under "Experimental Procedures." Immunoblots were stained with a monoclonal antibody against the HA epitope to detect HA-tagged Pma1p and with polyclonal antibodies against the GPI-anchored protein, Gas1p, or the *medial*-Golgi v-SNARE, Gos1p. The density profiles were similar for all gradients (not shown).

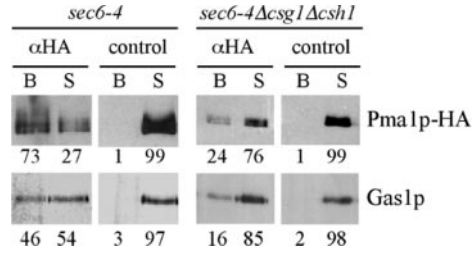

FIG. 11. **Pma1p and Gas1p are packaged into a common secretory vesicle species.** Aliquots from the PM-ATPase peak fractions derived from temperature-shifted, Pma1p-HA-expressing *sec6-4* or *sec6-4Δcsg1Δcsh1* cells (Fig. 10) were used to immunoisolate Pma1p-containing vesicles with anti-HA monoclonal antibodies (αHA) bound to Dynabeads protein G. Immunoisolations with Dynabeads containing anti-Myc monoclonal antibodies served as control. The percentage of immunopreciptated Pma1p and Gas1p was determined by Western blot analysis. *B*, beads; *S*, supernatant.

the first committed step of sphingolipid synthesis (22). Precisely what structural determinants on sphingolipids are critical for a correct delivery of cell surface components has remained an open issue. The availability of a yeast strain with a primary block in IPC mannosylation led us to investigate whether maturation of the sphingolipid head group serves a role in organizing membrane trafficking to the plasma membrane.

Yeast harbors two transport routes from the Golgi to the plasma membrane. One route mediates delivery of Pma1p while the other one carries the secretory enzyme invertase among its cargo (7). Our data show that the GPI-anchored protein, Gas1p, segregates from the invertase route and is packaged with Pma1p into a common transport carrier for delivery to the plasma membrane. Blocking sphingolipid mannosylation by disrupting *CSG1* and *CSH1* had no effect on the sorting of these cargo molecules and we observed that temperature-shifted *sec6-4Δcsg1Δcsh1* cells accumulate two population of secretory vesicles with characteristics indistinguishable from those generated in *sec6-4* cells. Moreover, thin-section electron microscopy revealed that both cell types accumulate very similar amounts of secretory vesicles (data not shown). Hence, mannosylated sphingolipids appear fully dispensable for the biogenesis of the two classes of secretory vesicles that mediate cell surface transport in yeast.

Also transport through the Golgi seems unaffected by a block in sphingolipid mannosylation. This can be inferred from the fact that *Δcsg1Δcsh1* cells deliver newly synthesized vacuolar proteins at wild-type kinetics and do not contain higher levels of Golgi-modified invertase than wild-type cells. Collectively, our data indicate that the plasma membrane trafficking defects previously reported for mutants blocked in the first committed step of sphingolipid synthesis cannot be ascribed to a deficiency in complex mannosylated sphingolipids (17–19). In fact, we found no evidence for a critical function of mannosylated sphingolipids in any of the known post-Golgi delivery pathways in yeast.

It has been shown that GDP-mannose transport into the Golgi lumen is essential for cell growth (24). Since mannosylation of proteins in the Golgi does not appear to be essential, it has been suggested that the strict requirement of GDP-mannose transport involves its effect on sphingolipid mannosylation (24). This idea is inconsistent with our present findings. Mannosylated sphingolipids are abundant components of the yeast plasma membrane, accounting for up to 8% of its total mass (25, 52). Therefore, it is somewhat surprising that a complete block in their synthesis has little if any effect on cell growth, at least under standard growth conditions (YEPD or synthetic medium at 30 °C). Strains deleted for *CSG1* are hypersensitive for calcium (27) and we and others (29) found that this phenotype is aggravated upon additional loss of *CSH1*. This calcium sensitivity is likely due to accumulation and/or mislocalization of IPC (more specifically IPC-C) rather than depletion of MIPC or $M(IP)_2C$ (27). Interestingly, recent work suggests that $M(IP)_2C$ synthesis is controlled in coordination with multidrug resistance in yeast, and that this lipid serves a role in determining the activity of drug transporters in and/or the permeability properties of the plasma membrane (53). How mannosylated sphingolipids contribute to the functional orga-

nization of the plasma membrane poses an intriguing problem for future research.

Acknowledgments—We thank Edina Harsay, Amy Chang, Howard Riezman, Sirkka Keränen, Timothy Levine, Ben Nichols, Sean Munro, and Steve Nothwehr for generously providing strains, plasmids or antibodies, to Sigrún Hrafnsdóttir and Juergen Stolz for helpful advice, and to Maurice Jansen for expert technical assistance.

REFERENCES

1. Mellman, I. (1996) *Annu. Rev. Cell Dev. Biol.* **12,** 575–625
2. Burd, C. G., Babst, M., and Emr, S. D. (1998) *Semin. Cell Dev. Biol.* **9,** 527–533
3. Keller, P., and Simons, K. (1997) *J. Cell Sci.* **110,** 3001–3009
4. Mostov, K. E., Verges, M., and Altschuler, Y. (2000) *Curr. Opin. Cell Biol.* **12,** 483–490
5. Yoshimori, T., Keller, P., Roth, M. G., and Simons, K. (1996) *J. Cell Biol.* **133,** 247–256
6. Musch, A., Xu, H., Shields, D., and Rodriguez-Boulan, E. (1996) *J. Cell Biol.* **133,** 543–558
7. Harsay, E., and Bretscher, A. (1995) *J. Cell Biol.* **131,** 297–310
8. David, D., Sundarababu, S., and Gerst, J. E. (1998) *J. Cell Biol.* **143,** 1167–1182
9. Harsay, E., and Schekman, R. (2002) *J. Cell Biol.* **156,** 271–285
10. Brown, D. A., and London, E. (2000) *J. Biol. Chem.* **275,** 17221–17224
11. van Meer, G., Stelzer, E. H. K., Wijnaendts-van-Resandt, R. W., and Simons, K. (1987) *J. Cell Biol.* **105,** 1623–1635
12. Simons, K., and van Meer, G. (1988) *Biochem.* **27,** 6197–6202
13. Mays, R. W., Siemers, K. A., Fritz, B. A., Lowe, A. W., van Meer, G., and Nelson, W. J. (1995) *J. Cell Biol.* **130,** 1105–1115
14. Ledesma, M. D., Simons, K., and Dotti, C. G. (1998) *Proc. Natl. Acad. Sci. U. S. A.* **95,** 3966–3971
15. Schmidt, K., Schrader, M., Kern, H. F., and Kleene, R. (2001) *J. Biol. Chem.* **276,** 14315–14323
16. Martin-Belmonte, F., Alonso, M. A., Zhang, X., and Arvan, P. (2000) *J. Biol. Chem.* **275,** 41074–41081
17. Skrzypek, M., Lester, R. L., and Dickson, R. C. (1997) *J. Bacteriol.* **179,** 1513–1520
18. Bagnat, M., Keranen, S., Shevchenko, A., and Simons, K. (2000) *Proc. Natl. Acad. Sci. U. S. A.* **97,** 3254–3259
19. Bagnat, M., Chang, A., and Simons, K. (2001) *Mol. Biol. Cell* **12,** 4129–4138
20. Sprong, H., Degroote, S., Claessens, T., van Drunen, J., Oorschot, V., Westerink, B. H., Hirabayashi, Y., Klumperman, J., van der Sluijs, P., and van Meer, G. (2001) *J. Cell Biol.* **155,** 369–380
21. Merrill Jr., A. H., and Sweeley, C. C. (1996) in *Biochemistry of Lipids, Lipoproteins and Membranes* (Vance, D., and Vance, J. E., eds) pp. 309–339, Elsevier, Amsterdam
22. Dickson, R. C., and Lester, R. L. (1999) *Biochim. Biophys. Acta* **1438,** 305–321
23. Levine, T. P., Wiggins, C. A., and Munro, S. (2000) *Mol. Biol. Cell* **11,** 2267–2281
24. Dean, N., Zhang, Y. B., and Poster, J. B. (1997) *J. Biol. Chem.* **272,** 31908–31914
25. Hechtberger, P., Zinser, E., Saf, R., Hummel, K., Paltauf, F., and Daum, G. (1994) *Eur. J. Biochem.* **225,** 641–649
26. Beeler, T., Gable, K., Zhao, C., and Dunn, T. (1994) *J. Biol. Chem.* **269,** 7279–7284
27. Beeler, T. J., Fu, D., Rivera, J., Monaghan, E., Gable, K., and Dunn, T. M. (1997) *Mol. Gen. Genet.* **255,** 570–579
28. Tanida, I., Takita, Y., Hasegawa, A., Ohya, Y., and Anraku, Y. (1996) *FEBS Lett.* **379,** 38–42
29. Uemura, S., Kihara, A., Inokuchi, J. I., and Igarashi, Y. (2003) *J. Biol. Chem.* **278,** 45049–45055
30. Elble, R. (1992) *BioTechniques* **13,** 18–20
31. Holthuis, J. C. M., Nichols, B. J., and Pelham, H. R. B. (1998) *Mol. Biol. Cell* **9,** 3383–3397
32. Jungmann, J., Rayner, J. C., and Munro, S. (1999) *J. Biol. Chem.* **274,** 6579–6585
33. Sauer, B. (1987) *Mol. Cell Biol.* **7,** 2087–2096
34. Wach, A., Brachat, A., Alberti-Segui, C., Rebischung, C., and Philippsen, P. (1997) *Yeast* **13,** 1065–1075
35. Ziman, M., Chuang, J. S., and Schekman, R. W. (1996) *Mol. Biol. Cell* **7,** 1909–1919
36. Sikorski, R. S., and Hieter, P. (1989) *Genetics* **122,** 19–27
37. Bonner, W. M., and Stedman, J. D. (1978) *Anal. Biochem.* **89,** 247–256
38. Holthuis, J. C. M., Nichols, B. J., Dhruvakumar, S., and Pelham, H. R. (1998) *EMBO J.* **17,** 113–126
39. Nakayama, K., Nagasu, T., Shimma, Y., Kuromitsu, J., and Jigami, Y. (1992) *EMBO J.* **11,** 2511–2519
40. Wiggins, C. A., and Munro, S. (1998) *Proc. Natl. Acad. Sci. U. S. A.* **95,** 7945–7950
41. Haak, D., Gable, K., Beeler, T., and Dunn, T. (1997) *J. Biol. Chem.* **272,** 29704–29710
42. Ziegler, F. D., Maley, F., and Trimble, R. B. (1988) *J. Biol. Chem.* **263,** 6986–6992
43. Rayner, J. C., and Munro, S. (1998) *J. Biol. Chem.* **273,** 26836–26843
44. Nagiec, M. M., Nagiec, E. E., Baltisberger, J. A., Wells, G. B., Lester, R. L., and Dickson, R. C. (1997) *J. Biol. Chem.* **272,** 9809–9817
45. Stack, J. H., DeWald, D. B., Takegawa, K., and Emr, S. D. (1995) *J. Cell Biol.* **129,** 321–334
46. Cowles, C. R., Snyder, W. B., Burd, C. G., and Emr, S. D. (1997) *EMBO J.* **16,** 2769–2782
47. Gurunathan, S., David, D., and Gerst, J. E. (2002) *EMBO J.* **21,** 602–614
48. TerBush, D. R., Maurice, T., Roth, D., and Novick, P. (1996) *EMBO J.* **15,** 6483–6494
49. Puoti, A., Desponds, C., and Conzelmann, A. (1991) *J. Cell Biol.* **113,** 515–525
50. Brown, D. A., and Rose, J. K. (1992) *Cell* **68,** 533–544
51. Simons, K., and Ikonen, E. (1997) *Nature* **387,** 569–572
52. Patton, J. L., and Lester, R. L. (1991) *J. Bacteriol.* **173,** 3101–3108
53. Hallstrom, T. C., Lambert, L., Schorling, S., Balzi, E., Goffeau, A., and Moye-Rowley, W. S. (2001) *J. Biol. Chem.* **276,** 23674–23680
54. Stepp, J. D., Huang, K., and Lemmon, S. K. (1997) *J. Cell Biol.* **139,** 1761–1774